

RESEARCH ARTICLE

BIOSYNTHESIS AND CHARACTERIZATION OF COPPER (II) OXIDE NANOPARTICLES USING NEEM LEAF EXTRACT FOR PHOTOCATALYTIC APPLICATIONS

Babatola, Babatude Keji^a, Adebayo, Samuel^b, Abiona, Mujidat Ayobami, Ajide, Adeolu Bamidele^d

^aScience Laboratory Technology Department, Osun State Polytechnic, Iree, Nigeria

^bPhysics Department, University of Ilorin, Ilorin Nigeria

^cApplied Science Department, Osun State Polytechnic, Iree, Nigeria

^dPhysics Department, University of Uyo, Uyo, Nigeria.

*Corresponding author email: samadeyemi29@gmail.com

This is an open access journal distributed under the Creative Commons Attribution License CC BY 4.0, which permits unrestricted use, distribution, and reproduction in any medium, provided the original work is properly cited.

ARTICLE DETAILS

Article History:

Received 10 January 2025

Revised 15 February 2025

Accepted 13 March 2025

Available online 09 April 2025

ABSTRACT

Copper (II) oxide nanoparticles (CuO-NPs) are gaining significant attention due to their unique properties and applications in various fields, including photocatalysis, environmental remediation, and sensors. The biosynthesis of CuO-NPs offers an eco-friendly and cost-effective approach compared to traditional chemical synthesis methods. Neem leaf extract, known for its reducing and stabilizing properties, serves as an ideal candidate for nanoparticle synthesis. This study aims to biosynthesize CuO-NPs using copper acetate monohydrate as a precursor and neem leaf (*Azadirachta indica*) extract as a reducing and stabilizing agent, followed by a thorough characterization of the synthesized nanoparticles. CuO-NPs were synthesized by mixing copper acetate monohydrate with neem leaf extract, followed by annealing at 400°C for one hour. The synthesized nanoparticles were characterized using several techniques: X-ray diffraction (XRD) for structural analysis, Fourier-transform infrared (FTIR) spectroscopy for functional group analysis, UV-Visible spectroscopy for optical properties, and atomic absorption spectroscopy (AAS) to determine copper concentration. XRD analysis confirmed the formation of CuO nanoparticles with a monoclinic crystal structure, with crystallite sizes of 49.62 nm for sample A and 55.95 nm for sample B. FTIR spectra exhibited peaks at 516.92 cm⁻¹, 518.85 cm⁻¹, and 617.22 cm⁻¹, indicating successful nanoparticle formation. AAS analysis revealed copper concentrations of 0.44 mg/L and 0.40 mg/L for samples A and B, respectively. The UV-Visible spectra indicated direct energy band gaps of 1.75 eV for sample A and 2.25 eV for sample B. The findings highlight the successful synthesis of CuO-NPs with desirable structural and optical properties. The energy band gaps suggest potential for photocatalytic applications, and the presence of functional groups confirmed nanoparticle formation. This study successfully demonstrates the biosynthesis of CuO-NPs using neem leaf extract. The synthesized nanoparticles show promising structural and optical characteristics, indicating their potential use in environmental and energy applications. The study presents an eco-friendly method for CuO-NP synthesis using neem leaf extract, highlighting its applicability for green synthesis and potential photocatalytic applications.

KEYWORDS

Atomic absorption spectroscopy (AAS), Energy band gap, Fourier transform infrared (FTIR) spectroscopy, UV-Visible spectroscopy, X-ray diffraction (XRD)

1. INTRODUCTION

Nanoparticle research has become a focal point in modern scientific advancements due to the unique properties of nanoparticles, such as enhanced electrical conductivity, improved hardness and ductility, better strength of metals and alloys, increased luminescent efficiency in semiconductors, and superior formability of ceramics (Rezić, 2022). These properties make nanoparticles particularly useful across various engineering, healthcare, agriculture, and environmental sciences applications. Among the numerous materials studied in nanoparticle research, copper oxide (CuO) nanoparticles have garnered significant attention for their exceptional characteristics. Copper (Cu) is a transition metal belonging to Group 11 (IB) in the periodic table, while oxygen (O) is a chalcogen element from Group 16 (VIA), period 2 (Siddiqi and Husen, 2020; Cuong et al., 2021). Copper oxide (CuO), also known as tenorite or

cupric oxide, is a Group II-VI metal oxide semiconductor. The visible form of CuO nanoparticles is typically a brownish-black powder. CuO nanoparticles can be reduced to metallic copper under high temperatures by reducing agents such as hydrogen, carbon monoxide (CO), or carbon (Mandal et al., 2018). Despite their promising potential, CuO nanoparticles are classified as harmful to aquatic life, the environment, and human health.

Advances in material science and engineering have primarily driven the rapid technological evolution of modern society. The discovery and synthesis of novel materials with remarkable physicochemical and mechanical properties are essential for the ongoing development of contemporary technology (Khan et al., 2019). This has been particularly evident in optoelectronics and photovoltaic cell industries. In today's world, thin films and nanomaterials are required to advance these

Quick Response Code



Access this article online

Website:
www.actachemicamalaysia.com

DOI:
10.26480/acmy.01.2025.70.76

industries, which play a key role in developing solar cells, sensors, and other high-tech applications. Alongside these, nanomaterials have wide-ranging uses in different sectors, such as healthcare, agriculture, and environmental sustainability (Chen et al., 2021). A central area of interest in material science is semiconductors, which are crucial for electronic devices. Unlike metals and insulators, semiconductors exhibit electrical conductivity that can be controlled by doping with other materials, making them highly versatile (Song et al., 2024). Semiconductors can be classified into two categories based on their band-gap structure: direct and indirect band-gap semiconductors. Silicon, one of the most studied semiconducting materials, is an indirect band-gap semiconductor and remains at the forefront of electronics and photovoltaic technologies (Huo et al., 2024). However, the limitations of silicon, such as its inefficiency in optical systems and its performance degradation when exposed to radiation over extended periods, have driven the search for new materials that can offer better performance in high-efficiency devices.

Chalcogenides, chalcopyrites, and metal oxide semiconductors doped with rare-earth and transition metals have emerged as promising alternatives. These materials show particular promise in optoelectronic devices such as solar cells, displays, and photodetectors (Priyadarshini et al., 2022). They also hold potential for other applications like gas sensors and photonics, essential for advancing modern technology. The synthesis and development of materials with specific properties often rely on precise control over the material's microstructure and the methods used to produce them. The processes used to create these materials must be carefully optimized to achieve the desired characteristics (Nikolic et al., 2020). Nanotechnology and thin film technology are key to building materials that exhibit physical, chemical, and functional properties that deviate significantly from the corresponding bulk properties of the material. These unique properties are particularly valuable in advanced applications such as nanoelectronics, energy conversion, catalysis, environmental protection, and space exploration (Banin et al., 2020).

Nanomaterials are typically measured on the nanoscale (1 to 100 nanometers) with their unique chemical and physical properties. At this scale, materials behave very differently from their bulk counterparts. Nanomaterials exhibit enhanced surface-to-volume ratios, which can significantly improve properties such as strength, reactivity, and conductivity. The development of these materials has been made possible by advances in various scientific disciplines, including surface engineering, plasma physics, solid-state physics, and computational chemistry (Saleh, 2020). Nanotechnology has emerged as one of the most significant technological advancements of the 21st century. It spans physics, chemistry, biology, material science, and medicine and is rapidly evolving as a multidisciplinary field (Kolahalam et al., 2019). The term "nano" refers to materials that are on the order of one billionth of a meter (10^{-9} m), and the prefix "nanos" is derived from the Greek word for "dwarf." Physicist Richard Feynman formally introduced the field of nanotechnology in his 1959 lecture titled "There's Plenty of Room at the Bottom," where he outlined the potential for manipulating matter on an atomic and molecular scale. Since then, nanotechnology has witnessed significant growth in research and application, with numerous breakthroughs in developing innovative nanoscale materials.

One of the most critical advances in nanotechnology has been the creation of copper oxide (CuO) nanoparticles. CuO nanoparticles possess unique optical, electrical, and chemical properties, making them ideal candidates for various applications, such as solar cells, sensors, photocatalysis, and environmental remediation (Cuong et al., 2021). Their synthesis, characterization, and potential applications have been the subject of numerous studies, focusing on their behaviour in various environments, including their ability to interact with light and electricity. The research into copper oxide nanoparticles is particularly relevant due to their potential in energy applications (Majumdar and Ghosh, 2020). As semiconductors, CuO nanoparticles can be used in developing high-efficiency solar cells, where their ability to absorb light and convert it into electrical energy is key to improving the performance of solar energy technologies. CuO nanoparticles have shown promise in photocatalytic applications, where they can facilitate chemical reactions, such as the degradation of pollutants, in the presence of light (Kumar et al., 2023). CuO nanoparticles also have significant applications in sensor technologies, particularly gas sensors. Their unique ability to interact with gases and undergo changes in electrical conductivity makes them highly suitable for detecting a range of gases, including toxic or hazardous gases (Lupan et al., 2020). This property has led to the exploration of CuO nanoparticles in environmental monitoring and safety applications.

Developing copper oxide nanoparticles represents a significant advancement in material science and nanotechnology. Their unique properties, including their behaviour as semiconductors, their ability to interact with light and electricity, and their potential applications in

energy, environmental, and sensor technologies, make them highly promising for future technological innovations (Luque-Jacobo et al., 2023). As research in this field continues to evolve, it is expected that CuO nanoparticles will play an increasingly important role in addressing modern society's challenges, particularly in energy production, environmental sustainability, and safety. The continued development of nanomaterials like CuO nanoparticles will be crucial in advancing technologies that improve society and the environment.

2. METHODOLOGY

Copper (II) oxide nanoparticles were biosynthesized using Copper(II) acetate monohydrate ($(CH_3COO)_2Cu \cdot H_2O$) of analytical grade (98%, MW = 199.65 g/mol), purified water, and neem leaf (*Azadirachta indica*) extract as a reducing and stabilizing agent. Neem leaves were collected, thoroughly washed with distilled water to remove dust, and dried (Gopalakrishnan and Muniraj, 2020). The dried leaves were ground into a fine powder using a blender and stored in an airtight container. To prepare the neem leaf extract, 5g of the powdered neem leaves were added to 500ml of purified water. The mixture was heated in a water bath at 80°C until the colour changed from pale yellow to light amber. After cooling, the filtrate was collected by filtering through paper and stored for further use.

To biosynthesize the copper (II) oxide nanoparticles, 1g of Copper(II) acetate was mixed with 500 ml of the neem leaf extract solution, and 8g of Copper(II) acetate was combined with 80 ml of the extract. The resulting paste was placed in a ceramic crucible and heated for an hour at 400°C in an air-heated furnace (Gopalakrishnan and Muniraj, 2020). After cooling, a deep black powder was obtained, carefully collected and stored. The powder was further processed by grinding it with a spatula in a ceramic crucible to achieve a finer consistency for characterization. The resulting copper (II) oxide nanoparticles were analyzed using UV-visible, FTIR, XRD, and AAS techniques for further characterization, as described in previous studies on copper nanoparticle biosynthesis (Copper Metal Nanoparticle Biosynthesis and Characterization Using Ascorbic Acid, 2015).

2.1 Characterization

After an hour of annealing, UV-visible spectroscopy Analysis was performed to monitor the reduction of Cu^{2+} ions to CuO nanoparticles in the reaction medium. The UV-visible spectra were measured to track the process. X-ray Diffraction (XRD) Analysis was conducted using an EMPYREAN X-ray diffractometer equipped with a graphite monochromator, employing Cu-K radiation. XRD patterns were generated to determine the crystallite size, identify the peaks with the highest intensities, and assess the type of crystal structure, lattice constants, and compound type, following the methodology of (Guo et al., 2020).

The synthesis of the metal oxide nanoparticles was further analyzed using Atomic Absorption Spectrometry (AAS) and Fourier Transform Infrared Spectroscopy (FTIR). FTIR spectra were obtained with a SHIMADZU Model 8400S spectrophotometer (Japan) at a resolution of 4 cm^{-1} with 64 co-added scans, covering the range of 500 cm^{-1} to 4000 cm^{-1} . AAS was performed using a BUCK Scientific ACCUSYS 211 spectrophotometer to determine the elemental composition of metals in the compounds expressed in concentration (mg/L). Prior to AAS analysis, the samples were digested by adding 1g of CuO nanoparticles into a digestion flask, followed by 9 ml of concentrated HNO_3 and 3 ml of concentrated HCl (3:1 ratio). The samples were heated on a hot plate until all brown fumes were expelled. After digestion, the mixtures were filtered and diluted with distilled water for AAS analysis. Data collected from UV-visible and FTIR spectrophotometric measurements were analyzed using Origin 8 Pro Version Software to interpret the findings.

3. RESULTS AND DISCUSSION

3.1 Result

The UV-Visible absorption spectra of Copper (II) Oxide (CuO) nanoparticles (NPs) synthesized in two different samples have been analyzed to understand their potential applications in solar cells and as photocatalytic agents. CuO nanoparticles have garnered significant attention due to their optical properties, which make them suitable for a variety of applications, including solar energy harvesting and environmental remediation (Alzalzala and Al-Shamari, 2023). In this study, the UV-Visible spectra of CuO NPs in Sample 1 and Sample 2 are

discussed, revealing important characteristics such as absorption peaks, transmittance properties, energy band gaps, and crystallinity, which support their potential for use in solar cells and wastewater purification.

3.1.1 UV-Visible Spectrum of CuO NPs in Sample 1

The UV-Visible spectrum of CuO nanoparticles in Sample 1 displayed a significant absorption peak at 580 nm in the visible region, as shown in Figure 1. This absorption peak suggests that CuO NPs in this sample absorb light effectively within the visible region, particularly at wavelengths around 580 nm within the range reported by (Chen et al., 2007). As the wavelength increases beyond this peak, the absorbance decreases, indicating a strong absorption in the visible region of the UV-Visible spectrum (200-700 nm, Jia et al., 2022).

Table 1: The crystallite size of CuO NPs in Sample 1.					
2 θ (degree) JCPDS Card	2 θ (degree) Observed	FWHM(β) (degree)	Crystallite size(D) (nm)	Preferred Crystal Orientation(hkl)	FWHM(β) (radians)
35.42	35.42	0.16	54.48	(002)	0.0028
38.71	38.76	0.18	48.86	(111)	0.0031
48.72	48.62	0.20	45.52	(-202)	0.0035

This characteristic makes CuO NPs in Sample 1 well-suited for use as an absorbing layer in solar cell materials. These materials can capture a broad range of solar radiation, making them an ideal candidate for enhancing the efficiency of solar cells by improving light absorption. The observed absorption spectrum indicates that CuO NPs in Sample 1 can function as effective photocatalysts, particularly for environmental applications such as the purification of wastewater. Photocatalysis involves the acceleration of a chemical reaction under light irradiation, and the high absorbance of CuO nanoparticles within the UV-Visible range suggests they could be used to degrade organic pollutants in contaminated water (Chauhan et al.,

2020).

Table 2: The crystallite size of CuO NPs in Sample 2					
2 θ (degree) JCPDS Card	2 θ (degree) Observed	FWHM(β) (degree)	Crystallite size(D) (nm)	Preferred Crystal Orientation(hkl)	FWHM(β) (radians)
35.54	35.70	0.14	62.26	(-111)	0.0024
38.71	38.70	0.16	55.01	(111)	0.0028
48.72	48.60	0.18	50.58	(-202)	0.0031

The surface plasmon resonance absorption in metal oxide nanoparticles like CuO is a characteristic feature that indicates the formation of nanoparticles in the solution. In the case of Sample 2, the CuO nanoparticles synthesized using neem leaf extract also demonstrated potential for use as an absorbing layer in solar cells. Like Sample 1, these nanoparticles can effectively absorb light within the UV-Visible range of 200-700 nm, making them suitable for solar energy applications. Furthermore, the strong absorption properties of CuO NPs in Sample 2 suggest that these nanoparticles could also be utilized as photocatalysts for the degradation of pollutants in wastewater.

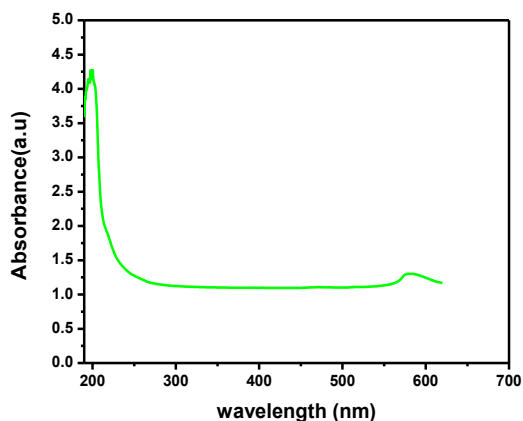


Figure 2: The UV-Visible Spectrum of Absorbance of CuO NPs in Sample

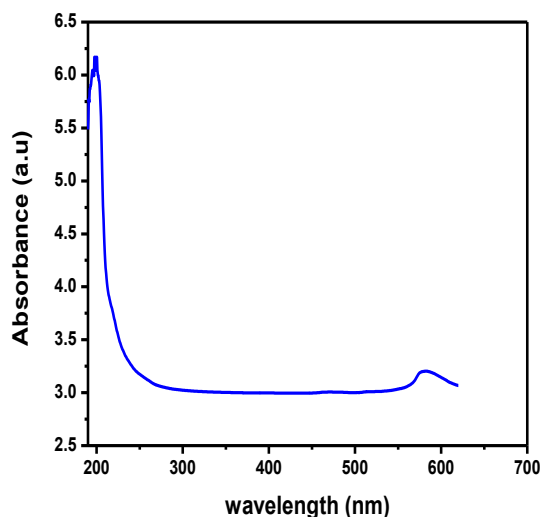


Figure 1 : shows the CuO nanoparticles in Sample 1's UV-visible spectrum of absorbance.

3.1.2 UV-Visible Spectrum of CuO NPs in Sample 2

In Sample 2, CuO nanoparticles were synthesized using an eco-friendly approach involving neem leaf (*Azadirachta indica*) extract dispersed in water. The UV-Visible spectrum of these nanoparticles also exhibited a peak at 580 nm, similar to that observed in Sample 1, as shown in Figure 2. The absorption peak at 580 nm is associated with the surface plasmon resonance of the CuO nanoparticles, a phenomenon resulting from the collective oscillation of free conduction band electrons upon interaction with incident electromagnetic radiation (Proença et al., 2019).

2.

3.1.3 Transmittance Spectrum of CuO NPs

The transmittance spectrum of CuO NPs in both Sample 1 and Sample 2 was analyzed to gain insight into the transparency and light transmission properties of the nanoparticles across the UV-Visible spectrum. The transmittance in both samples was observed to increase steadily until a constant value of transmittance was reached. However, there was a sharp increase in transmittance at approximately 550 nm, which indicates a significant change in the optical properties of the CuO nanoparticles around this wavelength. This increase in transmittance suggests that the CuO nanoparticles undergo a transition in their light absorption behavior, possibly due to changes in the electronic structure or the influence of surface states as the wavelength increases. Both samples exhibited this behavior, with Sample 1 showing a similar trend, making them suitable for potential photocatalytic applications, particularly in environmental cleanup, such as wastewater treatment. The steady increase in transmittance also indicates that after reaching a certain threshold wavelength, the material does not absorb light as effectively, thus contributing to the transparency or optical transparency of the material at those wavelengths (Wu et al., 2021).

The significant changes in transmittance and absorption observed in the UV-Visible spectra are indicative of the potential for CuO NPs to be utilized in various applications. As photocatalysts, the ability to absorb light effectively and then transmit certain wavelengths is crucial for facilitating photochemical reactions (Sharma et al., 2021). The decrease in absorption with increasing wavelength suggests that CuO nanoparticles can be tailored for specific wavelength ranges, which is a valuable property for optimizing the material's use in solar cells and photocatalytic processes (Atta et al., 2023).

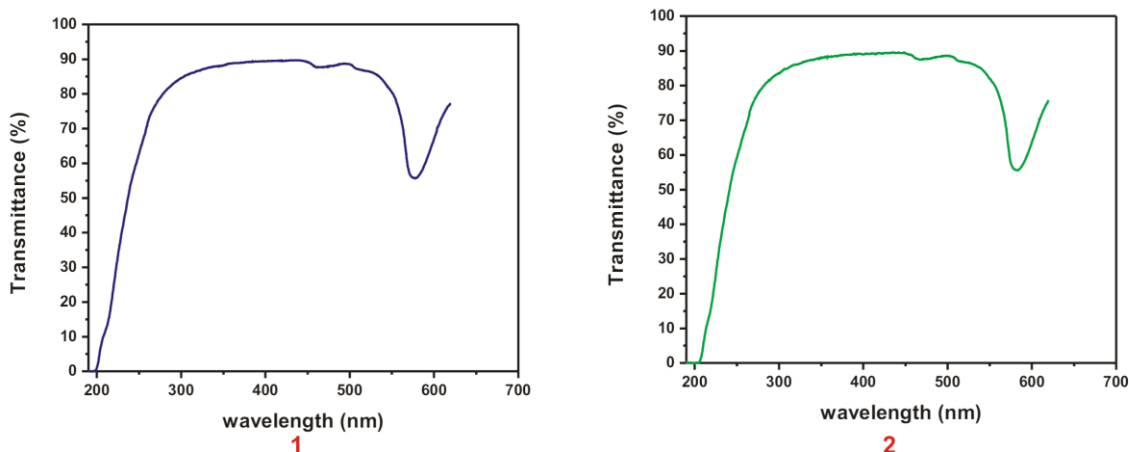


Figure 3: shows the transmittance of CuO NPs in Samples 1 and 2 over the UV-visible spectrum.

3.1.4 Direct Energy Band Gaps of CuO NPs

The direct energy band gaps of CuO NPs in Sample 1 and Sample 2 were calculated and analyzed to understand their electronic properties and their suitability for applications in energy harvesting and catalysis. The band gap is a critical property that determines the material's electronic behavior and its ability to absorb light at specific wavelengths. CuO is a semiconductor with a relatively wide band gap, and this property influences its photocatalytic behavior and its application in solar energy systems (Balik et al., 2018).

Table 3: Variation of Observed lattice constant with Standard lattice constant					
2 θ (degree)	Crystal Orientation (hkl)	θ (degree)	d-spacing (Å)	Observed lattice constant (Å)	Standard lattice constant (Å)
38.90	(200)	19.45	2.313	a=4.626	a=4.6837
53.49	(020)	26.75	1.711	b=3.422	b=3.4226
35.42	(002)	17.71	2.532	c=5.064	c=5.1288

In Sample 1, the direct energy band gap of the CuO nanoparticles was red-

shifted due to surface imperfections. Surface defects and disorder in nanoparticles can lead to changes in their electronic structure, causing a shift in the band gap. This red shift implies that the material's ability to absorb lower-energy photons is enhanced, making it useful for capturing a broader range of sunlight, including in the visible spectrum (Sahu et al., 2020). In contrast, the direct band gap in Sample 2 was observed to be larger due to the quantum confinement effect. Quantum confinement occurs when the size of nanoparticles is reduced to the point where electronic properties such as the band gap are significantly altered. This effect results in an increased band gap and, in turn, a shift toward the absorption of higher-energy photons (Zwijenburg, 2022). The larger band gap in Sample 2 suggests that the CuO nanoparticles may be more efficient at absorbing higher-energy UV radiation, which is beneficial for both solar cell applications and photocatalytic processes.

The comparison between the two samples indicates that both have distinct advantages depending on the application. Sample 1, with its red-shifted band gap, may be more suitable for solar energy applications, particularly in environments with abundant visible light. On the other hand, Sample 2, with its larger band gap, could be more efficient in environments where UV light is more prevalent, or for processes that require higher-energy photon absorption.

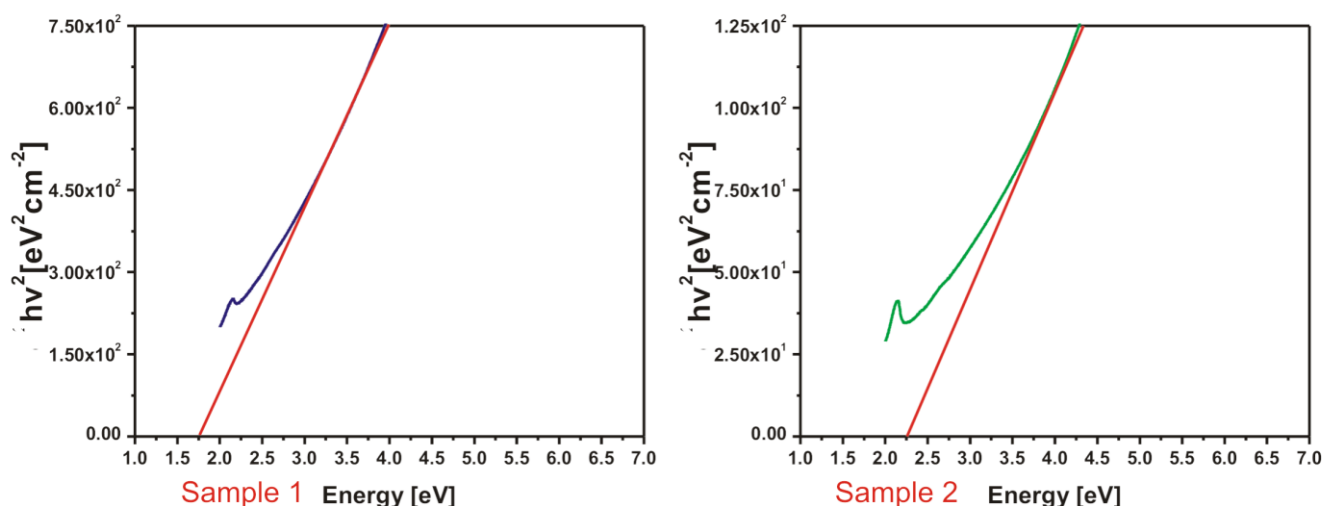


Figure 4: CuO NPs in Samples 1 and 2's Direct Energy Band Gap

3.1.5 X-Ray Diffraction (XRD) Analysis of CuO NPs

To further characterize the structural properties of the CuO nanoparticles, X-Ray Diffraction (XRD) analysis was performed on both Sample 1 and Sample 2. XRD patterns are essential for determining the crystallinity and phase structure of nanoparticles. Figure 5 shows the typical XRD patterns

of CuO nanoparticles from both samples. The XRD patterns exhibited peaks corresponding to the monoclinic crystal structure of CuO, which is the characteristic phase of Copper (II) Oxide. The observed peaks confirmed that the nanoparticles synthesized in both samples were predominantly single-phase CuO, with no significant impurities or additional phases present (Baquer et al., 2017).

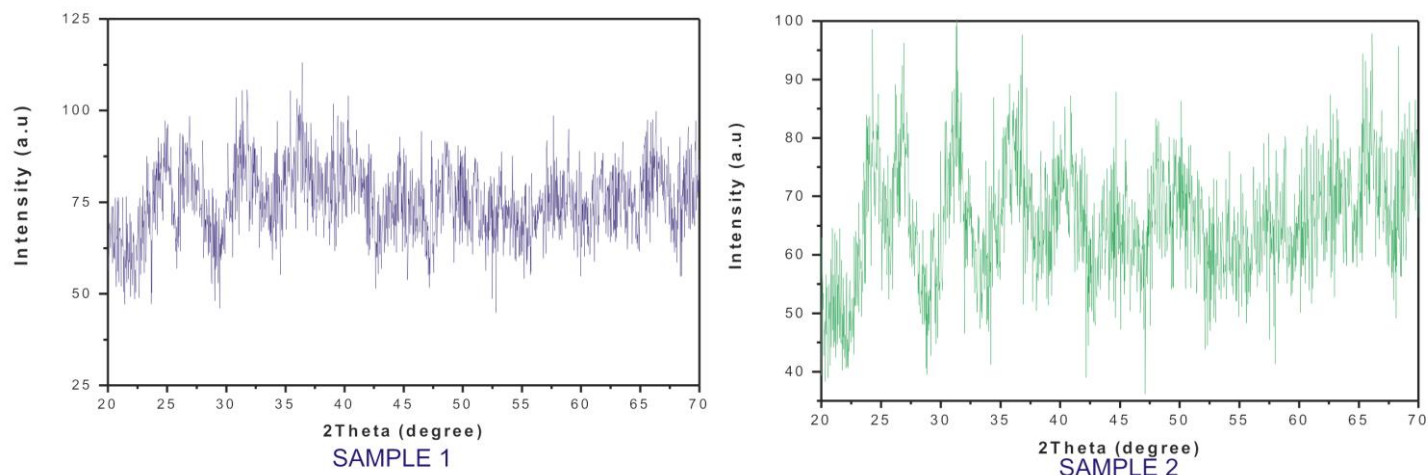


Figure 5: XRD pattern of CuO nanoparticles in Sample 1 and 2.

The XRD analysis also revealed that the crystallite size of the CuO nanoparticles in both samples was influenced by the annealing process. Sample 1 exhibited an average crystallite size of 49.62 nm, calculated using the Debye-Scherrer formula, which is based on the full width at half maximum (FWHM) of the XRD peaks. Sample 2 showed a slightly larger average crystallite size of 55.95 nm. The increase in crystallite size with annealing temperature is a common phenomenon, as higher temperatures allow for the growth of larger crystalline domains. This trend was observed in both samples, indicating that the annealing process had a significant effect on the crystallinity of the CuO nanoparticles. The XRD data for both samples were compared to reference values from the Joint Committee on Powder Diffraction Standards (JCPDS), which confirmed that the observed lattice constants were in good agreement with the standard values for CuO (Srivastava, 2013).

The crystallite size and lattice parameters of CuO nanoparticles are crucial for determining their optical and electronic properties. The larger crystallite size observed in Sample 2 suggests that the nanoparticles in this sample may have improved structural integrity and enhanced stability, which could be beneficial for photocatalytic and solar cell applications (Kamble and Mote, 2021). Larger crystals often result in fewer surface defects and improved charge carrier mobility, which can enhance the efficiency of energy conversion and photocatalysis.

4. CONCLUSION

This study presents an in-depth analysis of the UV-visible spectra, transmittance, energy band gaps, and crystallite sizes of Copper (II) Oxide nanoparticles (CuO NPs) synthesized using two different methods: one utilizing a direct synthesis technique and the other incorporating neem leaf (*Azadirachta indica*) extract as a green reducing agent. The study's findings suggest that CuO NPs synthesized from both methods exhibit promising characteristics for various applications, particularly in solar cells and photocatalysis.

4.1 UV-Visible Absorption Behavior of CuO NPs

The UV-visible absorption spectra of CuO NPs in samples 1 and 2, displayed in Figures 1 and 2, show a strong absorption peak at 580 nm in the visible region. This absorption peak is consistent with reports in the literature for CuO NPs, which typically exhibit an absorption band around 580 nm, attributed to surface plasmon resonance (SPR) (Kazuma et al., 2011). The absorption peak of 580 nm in both samples suggests that these nanoparticles have excellent light-absorbing properties within the UV-visible range of 200-700 nm. This characteristic is crucial for applications in solar energy conversion, specifically as an absorbing layer in solar cells.

The decrease in absorbance with increasing wavelength within the UV-visible range is typical behaviour for metal oxide nanoparticles, where the absorption efficiency diminishes as the wavelength increases (Duque et al., 2019). This decrease indicates the material's selective absorption properties, absorbing more light at shorter wavelengths while transmitting longer wavelengths. Therefore, the CuO NPs in both samples show the potential to function effectively as light-harvesting materials in solar cells, capturing energy in the UV and visible regions of the solar spectrum. Furthermore, CuO NPs are known for their photocatalytic properties, which make them suitable for environmental applications, such as wastewater purification (Siddiqi and Husen, 2020). The absorption characteristics observed in this study suggest that CuO NPs in

both samples could be employed for photocatalytic degradation of organic pollutants under UV and visible light exposure.

4.1.1 Transmittance Spectra and Photocatalytic Potential

Figure 3 illustrates the transmittance spectra of CuO NPs in samples 1 and 2 over the UV-visible region. It is evident from the spectra that the transmittance increases until it reaches a constant value, with a sharp increase observed at approximately 550 nm. This sharp rise in transmittance corresponds to the threshold wavelength at which the nanoparticles begin, allowing more light to pass through, commonly seen in semiconducting materials. The change in transmittance behaviour further corroborates the potential of these nanoparticles to act as efficient photocatalysts (Sarina et al., 2017). Photocatalysis requires the material to absorb light, generate electron-hole pairs, and degrade pollutants. The observed transmittance characteristics support the hypothesis that CuO NPs can perform this function effectively (Nazim et al., 2021).

Moreover, the transmittance data suggest that CuO NPs could be used for various photocatalytic applications, especially in environmental remediation, such as the degradation of organic contaminants in wastewater. The ability of CuO to absorb in the visible region, combined with its effective transmittance and photocatalytic behaviour, positions it as a potential material for developing more efficient and cost-effective photocatalysts for wastewater treatment (Bharti et al., 2020).

4.1.2 Energy Band Gap and Crystallinity

The energy band gaps of CuO NPs in samples 1 and 2 were analyzed and displayed in Figure 4. The band gap of the nanoparticles in sample 1 was red-shifted, likely due to surface defects or imperfections in the crystal structure. This red-shifting of the band gap is typical for nanoparticles, where the smaller particle size and surface states modify the electronic properties (Adesoye et al., 2022). In contrast, the energy band gap in sample 2 was higher, possibly due to quantum confinement effects, a known phenomenon in nanomaterials. The quantum confinement effect occurs when the particle size becomes small enough (typically below 10 nm) that the electronic energy levels begin to quantize, leading to a wider band gap (Ji et al., 2020).

The variation in energy band gaps between the two samples suggests that the method of synthesis (biosynthesis with neem leaf extract versus a direct chemical synthesis) influences the electronic properties of the CuO NPs. The smaller band gap in sample 1 implies that the nanoparticles may be more sensitive to visible light, enhancing their photocatalytic activity. In contrast, the more significant band gap in sample 2 could potentially result in improved stability and lower recombination rates of electron-hole pairs, which is also beneficial for photocatalytic applications (Zhou et al., 2018).

4.1.3 Crystallite Size and X-Ray Diffraction Analysis

X-ray diffraction (XRD) patterns were used to assess the crystallinity and phase structure of CuO NPs in both samples. Figures 5 and Tables 1 and 2 present the XRD data, indicating that both samples exhibit a monoclinic crystal structure consistent with the literature for CuO nanoparticles (Ahamed et al., 2014). The crystallite size of CuO NPs in sample 1 was calculated to be 49.62 nm, while in sample 2, it was slightly larger at 55.95 nm. The increase in crystallite size in sample 2 could be attributed to the biosynthesis process, where the presence of neem leaf extract as a

reducing agent may result in more considerable particle growth. The increase in particle size may also be linked to the annealing process, which promotes crystallization and grain growth (Ghosh et al., 2020).

The calculated crystallite sizes and the observed diffraction peaks suggest that the CuO NPs in both samples are crystalline and possess a stable monoclinic phase, which is essential for their application in solar cells and photocatalysis. Crystalline materials typically exhibit better charge carrier mobility, which enhances the efficiency of photocatalytic reactions and photovoltaic devices (Abdulnabi and Juda, 2023).

4.1.4 Comparison of Lattice Constants and Structural Properties

The variation of the observed lattice constant with the standard lattice constant, as shown in Table 3, reveals that the CuO NPs in both samples closely match the reference lattice values, further confirming the monoclinic crystal structure of the nanoparticles. The minor discrepancies between the observed and standard lattice constants could be attributed to slight strain or defects within the crystal structure, which can be a common feature of nanomaterials (Kamble and Mote, 2021). The lattice constants and the crystallite size data support the idea that CuO NPs synthesized through both methods exhibit a high degree of crystallinity, which is essential for photocatalytic applications, as crystalline materials typically exhibit better performance than amorphous ones.

The UV-visible spectra, transmittance characteristics, energy band gaps, and X-ray diffraction data presented in this study demonstrate that CuO nanoparticles synthesized using two different methods exhibit significant promise for solar energy harvesting and photocatalysis applications. Both samples of CuO NPs display a strong absorption peak at 580 nm, indicating their potential as absorbing layers in solar cells and as photocatalytic agents for wastewater purification. The crystallinity and size of the nanoparticles also play a crucial role in their photocatalytic activity and stability. The findings highlight the versatility of CuO nanoparticles and their potential to be employed in sustainable technologies for energy and environmental applications. Future work should explore the optimization of synthesis methods and the performance of CuO NPs in practical applications such as solar cells and wastewater treatment systems.

5. CONCLUSION

The present investigation discusses the biosynthesis and characterization of CuO-NPs using copper acetate monohydrate as a precursor and neem leaf (*Azadirachta indica*) as both a reducing and stabilizing agent. The resulting black paste was then annealed for a full hour at 400°C in the air, forming CuO nanoparticles. The synthesized CuO nanoparticles were crystalline, and XRD analysis revealed that the samples (1 and 2) exhibited single-phase monoclinic crystal structures with average crystallite sizes of 49.62 nm and 55.95 nm, respectively. This indicates the successful synthesis of CuO nanoparticles with well-defined crystalline properties. The optical properties of the CuO nanoparticles were examined using UV-visible absorption spectra. It was observed that CuO nanoparticles in sample B had a higher direct band gap than those in sample A, further confirming that the nanoparticles were crystalline. The direct band gap observed in both samples is relatively large, considering the size of the crystallites, suggesting their potential utility in various electronic and photonic applications. The presence of hydroxyl and carboxylate groups from the neem leaf extract facilitated the synthesis of copper hydroxide (Cu(OH)₂), which was subsequently hydrolyzed to form nano-crystalline CuO nanoparticles.

FTIR spectroscopy was employed to confirm the production of CuO nanoparticles, as the spectra displayed characteristic peaks corresponding to Cu-O bonds. AAS analysis revealed the copper metal concentration in the samples to be in the ratio of 0.44 mg/L in sample A and 0.40 mg/L in sample B, indicating the successful synthesis of CuO nanoparticles. These CuO nanoparticles have promising applications as photocatalytic agents, optoelectronic components, and solar cell technologies, owing to their unique optical and structural properties. Copper (II) oxide nanoparticles can be synthesized using neem leaf (*Azadirachta indica*) extract, offering a green, eco-friendly, and cost-effective method. These nanoparticles are valuable in organic-inorganic composites, photocatalysis, solar cells, and gas sensors. They also have antibacterial, antifungal, and biocide properties, making them useful in coatings, textiles, and wastewater treatment. CuO nanoparticles enhance electron field emission due to their low surface potential barrier.

REFERENCES

Abdulnabi, G., and Juda, A.M., 2023. Preparation and comparison performance of CuO Nanoparticles and CuO/TiO₂ / Nanocomposite and application in solar cell. *Journal of Kufa Physics*, 15 (01), Pp. 1–13. <https://doi.org/10.31257/2018/jkp/2023/v15.i01.10696>

- Adesoye, S., Abdullah, S.A., Nowlin, K., and Dellinger, K., 2022. Mg-Doped ZnO Nanoparticles with Tunable Band Gaps for Surface-Enhanced Raman Scattering (SERS)-Based Sensing. *Nanomaterials*, 12 (20), Pp. 3564. <https://doi.org/10.3390/nano12203564>
- Ahamed, M., Alhadlaq, H.A., Khan, M.A.M., Karuppiyah, P., and Al-Dhabi, N.A., 2014. Synthesis, Characterization, and Antimicrobial Activity of Copper Oxide Nanoparticles. *Journal of Nanomaterials*, 2014(1). <https://doi.org/10.1155/2014/637858>
- Alzalzala, S., and Al-Shamari, A.M.J., 2023. Preparation and Characterization of Copper Oxide CuO (II) nanoparticles Prepared by a Hydrothermal Method and for Solar Cells applications. *Journal of Kufa Physics*, 15 (02), Pp. 108–116. <https://doi.org/10.31257/2018/jkp/2023/v15.i02.12388>
- Atta, A., Abdeltwab, E., Negm, H., Alshammari, A.H., Abdelhamied, M.M., Ahmed, A.M., and Rabia, M., 2023. Boost the photocatalytic hydrogen production of the nanocomposites conducting polypyrrole modified with metal oxide (CuO). *Physica Scripta*, 98 (9), Pp. 095916. <https://doi.org/10.1088/1402-4896/accc18>
- Balık, M., Bulut, V., and Erdogan, I.Y., 2018. Optical, structural and phase transition properties of Cu₂O, CuO and Cu₂O/CuO: Their photoelectrochemical sensor applications. *International Journal of Hydrogen Energy*, 44 (34), Pp. 18744–18755. <https://doi.org/10.1016/j.ijhydene.2018.08.159>
- Banin, U., Waiskopf, N., Hammarström, L., Boschloo, G., Freitag, M., Johansson, E.M.J., Sá, J., Tian, H., Johnston, M.B., Herz, L.M., Milot, R.L., Kanatzidis, M.G., Ke, W., Spanopoulos, I., Kohlstedt, K.L., Schatz, G.C., Lewis, N., Meyer, T., Nozik, A.J., Brudvig, G. W., 2020. Nanotechnology for catalysis and solar energy conversion. *Nanotechnology*, 32 (4), Pp. 042003. <https://doi.org/10.1088/1361-6528/abbc8>
- Baqer, A.A., Matori, K.A., Al-Hada, N.M., Kamari, H.M., Shaari, A.H., Saion, E., and Chyi, J.L.Y., 2017. Copper oxide nanoparticles synthesized by a heat treatment approach with structural, morphological and optical characteristics. *Journal of Materials Science Materials in Electronics*, 29 (2), Pp. 1025–1033. <https://doi.org/10.1007/s10854-017-8002-3>
- Chauhan, M., Kaur, N., Bansal, P., Kumar, R., Srinivasan, S., and Chaudhary, G.R., 2020. Proficient Photocatalytic and Sonocatalytic Degradation of Organic Pollutants Using CuO Nanoparticles. *Journal of Nanomaterials*, Pp. 1–15. <https://doi.org/10.1155/2020/6123178>
- Chen, J., Zhou, Y., Fu, Y., Pan, J., Mohammed, O.F., and Bakr, O.M., 2021. Oriented Halide Perovskite Nanostructures and Thin Films for Optoelectronics. *Chemical Reviews*, 121 (20), Pp. 12112–12180. <https://doi.org/10.1021/acs.chemrev.1c00181>
- Chen, X.Y., Cui, H., Liu, P., and Yang, G.W., 2007. Shape-induced ultraviolet absorption of CuO shuttlelike nanoparticles. *Applied Physics Letters*, 90 (18), Pp. <https://doi.org/10.1063/1.2736285>
- Cuong, H.N., Pansambal, S., Ghotekar, S., Oza, R., Hai, N.T.T., Viet, N.M., and Nguyen, V., 2021. New frontiers in the plant extract mediated biosynthesis of copper oxide (CuO) nanoparticles and their potential applications: A review. *Environmental Research*, 203, 111858. <https://doi.org/10.1016/j.envres.2021.111858>
- Duque, J.S., Madrigal, B.M., Riascos, H., and Avila, Y.P., 2019. Colloidal Metal Oxide Nanoparticles Prepared by Laser Ablation Technique and Their Antibacterial Test. *Colloids and Interfaces*, 3 (1), Pp. 25. <https://doi.org/10.3390/colloids3010025>
- Ghosh, T., Chattopadhyay, A., Mandal, A.C., Pramanik, S., and Kuiri, P.K., 2020. Optical, structural, and antibacterial properties of biosynthesized Ag nanoparticles at room temperature using *Azadirachta indica* leaf extract. *Chinese Journal of Physics*, 68, Pp. 835–848. <https://doi.org/10.1016/j.cjph.2020.10.025>
- Gopalakrishnan, V., and Muniraj, S., 2020. Neem flower extract assisted green synthesis of copper nanoparticles – Optimisation, characterisation and anti-bacterial study. *Materials Today Proceedings*, 36, Pp. 832–836. <https://doi.org/10.1016/j.matpr.2020.07.013>
- Huo, S., Zhang, S., Wu, Q., and Zhang, X., 2024. Feature-Assisted Machine Learning for Predicting Band Gaps of Binary Semiconductors. *Nanomaterials*, 14 (5), Pp. 445. <https://doi.org/10.3390/nano14050445>
- Ji, B., Rabani, E., Efron, A.L., Vaxenburg, R., Ashkenazi, O., Azulay, D., Banin,

- U., and Millo, O., 2020. Dielectric Confinement and Excitonic Effects in Two-Dimensional Nanoplatelets. *ACS Nano*, 14 (7), Pp. 8257–8265. <https://doi.org/10.1021/acsnano.0c01950>
- Jia, X., Yin, S., and Tang, Z., 2022. A Simple Metamaterial for High-Performance Spectrum-Selective Absorption in the Visible Region. *Symmetry*, 14 (11), Pp., 2402. <https://doi.org/10.3390/sym14112402>
- Kamble, S.P., and Mote, V.D., 2021. Optical and room-temperature ferromagnetic properties of Ni-doped CuO nanocrystals prepared via auto-combustion method. *Journal of Materials Science Materials in Electronics*, 32 (5), Pp., 5309–5315. <https://doi.org/10.1007/s10854-020-05106-8>
- Kazuma, E., Yamaguchi, T., Sakai, N., and Tatsuma, T., 2011. Growth behaviour and plasmon resonance properties of photocatalytically deposited Cu nanoparticles. *Nanoscale*, 3(9)Pp. 3641. <https://doi.org/10.1039/c1nr10456j>
- Khan, K., Tareen, A. K., Aslam, M., Wang, R., Zhang, Y., Mahmood, A., Ouyang, Z., Zhang, H., and Guo, Z., 2019. Recent developments in emerging two-dimensional materials and their applications. *Journal of Materials Chemistry C*, 8(2)Pp.,387–440. <https://doi.org/10.1039/c9tc04187g>
- Kolahalam, L. A., Viswanath, I. K., Diwakar, B. S., Govindh, B., Reddy, V., and Murthy, Y., 2019. Review on nanomaterials: Synthesis and applications. *Materials Today Proceedings*, 18, 2182–2190. <https://doi.org/10.1016/j.matpr.2019.07.371>
- Kumar, B. A., Elangovan, T., Karthigaimuthu, D., Aravinth, D., Ramalingam, G., Ran, F., & Sangaraju, S., 2023. CdSe Quantum Dots Bedecked on ZnO/TiO₂/CuO Ternary Nanocomposite for Enhanced Photocatalytic and Photovoltaic Applications. *Langmuir*, 39(45)Pp., 15864–15877. <https://doi.org/10.1021/acs.langmuir.3c01428>
- Lupan, O., Ababii, N., Mishra, A. K., Gronenberg, O., Vahl, A., Schürmann, U., Duppel, V., Krüger, H., Chow, L., Kienle, L., Faupel, F., Adlung, R., De Leeuw, N. H., and Hansen, S., 2020. Single CuO/Cu₂O/Cu Microwire Covered by a Nanowire Network as a Gas Sensor for the Detection of Battery Hazards. *ACS Applied Materials & Interfaces*, 12(37)Pp., 42248–42263. <https://doi.org/10.1021/acsami.0c09879>
- Luque-Jacobo, C. M., Cespedes-Loayza, A. L., Echegaray-Ugarte, T. S., Cruz-Loayza, J. L., Cruz, I., De Carvalho, J. C., and Goyzueta-Mamani, L. D., 2023. Biogenic Synthesis of Copper Nanoparticles: A Systematic Review of Their Features and Main Applications. *Molecules*, 28(12)Pp., 4838. <https://doi.org/10.3390/molecules28124838>
- Majumdar, D., and Ghosh, S., 2020. Recent advancements of copper oxide based nanomaterials for supercapacitor applications. *Journal of Energy Storage*, 34, 101995. <https://doi.org/10.1016/j.est.2020.101995>
- Mandal, L., Yang, K. R., Motapothula, M. R., Ren, D., Lobaccaro, P., Patra, A., Sherburne, M., Batista, V. S., Yeo, B. S., Ager, J. W., Martin, J., and Venkatesan, T., 2018. Investigating the Role of Copper Oxide in Electrochemical CO₂ Reduction in Real Time. *ACS Applied Materials and Interfaces*, 10(10)Pp., 8574–8584. <https://doi.org/10.1021/acsami.7b15418>
- Nazim, M., Khan, A. P., Asiri, A. M., and Kim, J. H., 2021. Exploring Rapid Photocatalytic Degradation of Organic Pollutants with Porous CuO Nanosheets: Synthesis, Dye Removal, and Kinetic Studies at Room Temperature. *ACS Omega*, 6(4)Pp., 2601–2612. <https://doi.org/10.1021/acsomega.0c04747>
- Nikolic, M. V., Milovanovic, V., Vasiljevic, Z. Z., & Stamenkovic, Z., 2020. Semiconductor Gas Sensors: Materials, Technology, Design, and Application. *Sensors*, 20(22)Pp.,6694. <https://doi.org/10.3390/s20226694>
- Priyadarshini, P., Das, S., and Naik, R., 2022. A review on metal-doped chalcogenide films and their effect on various optoelectronic properties for different applications. *RSC Advances*, 12(16)Pp.,9599–9620. <https://doi.org/10.1039/d2ra00771a>
- Proença, M., Borges, J., Rodrigues, M. S., Meira, D. I., Sampaio, P., Dias, J. P., Pedrosa, P., Martin, N., Bundaleski, N., Teodoro, O. M., and Vaz, F., 2019. Nanocomposite thin films based on Au-Ag nanoparticles embedded in a CuO matrix for localized surface plasmon resonance sensing. *Applied Surface Science*, 484, 152–168. <https://doi.org/10.1016/j.apsusc.2019.04.085>
- Rezić, I., 2022. Nanoparticles for Biomedical Application and Their Synthesis. *Polymers*, 14(22)Pp., 4961. <https://doi.org/10.3390/polym14224961>
- Sahu, J., Soni, S., Kumar, S., Dalela, B., Alvi, P., Sharma, S., Phase, D., Gupta, M., Kumar, S., and Dalela, S., 2020. Defects and oxygen vacancies tailored structural, optical and electronic structure properties of Co-doped ZnO nanoparticle samples probed using soft X-ray absorption spectroscopy. *Vacuum*, 179, 109538. <https://doi.org/10.1016/j.vacuum.2020.109538>
- Saleh, T. A., 2020. Nanomaterials: Classification, properties, and environmental toxicities. *Environmental Technology and Innovation*, 20Pp., 101067. <https://doi.org/10.1016/j.eti.2020.101067>
- Sarina, S., Jaatinen, E., Xiao, Q., Huang, Y. M., Christopher, P., Zhao, J. C., and Zhu, H. Y., 2017. Photon Energy Threshold in Direct Photocatalysis with Metal Nanoparticles: Key Evidence from the Action Spectrum of the Reaction. *The Journal of Physical Chemistry Letters*, 8(11)Pp.,2526–2534. <https://doi.org/10.1021/acs.jpclett.7b00941>
- Sharma, S., Kumar, K., Thakur, N., Chauhan, S., and Chauhan, M. S., 2021. Eco-friendly *Ocimum tenuiflorum* green route synthesis of CuO nanoparticles: Characterizations on photocatalytic and antibacterial activities. *Journal of Environmental Chemical Engineering*, 9(4)Pp.,105395. <https://doi.org/10.1016/j.jece.2021.105395>
- Siddiqi, K. S., and Husen, A., 2020. Current status of plant metabolite-based fabrication of copper/copper oxide nanoparticles and their applications: a review. *Biomaterials Research*, 24(1)Pp., <https://doi.org/10.1186/s40824-020-00188-1>
- Siddiqui, H., Qureshi, M. S., and Haque, F. Z., 2020. Lithium-Doped CuO Nanosheets: Structural Transformation, Optical, and Electrical Characteristics with Enhanced Photocatalytic and Solar Cell Performance. *Energy & Environment Materials*, 4(4), 646–657. <https://doi.org/10.1002/eem2.12149>
- Song, S., Rahaman, M., and Jariwala, D., 2024. Can 2D Semiconductors Be Game-Changers for Nanoelectronics and Photonics? *ACS Nano*, 18(17)Pp., 10955–10978. <https://doi.org/10.1021/acsnano.3c12938>
- Srivastava, S., 2013. Synthesis and Characterisation of Copper Oxide nanoparticles. *IOSR Journal of Applied Physics*, 5(4), 61–65. <https://doi.org/10.9790/4861-0546165>
- Wu, Q., Zhou, J., Liu, X., Jiang, X., Zhang, Q., Lin, Z., and Xia, M. (2021). Ca₃(TeO₃)₂(MO₄) (M = Mo, W): Mid-Infrared Nonlinear Optical Tellurates with Ultrawide Transparency Ranges and Superhigh Laser-Induced Damage Thresholds. *Inorganic Chemistry*, 60(23)Pp.,18512–18520. <https://doi.org/10.1021/acs.inorgchem.1c03069>
- Zhou, B., Huang, W., Yang, K., Ding, S., Xie, Z., Pan, A., Hu, W., Peng, P., and Huang, G., 2018. Theory-Driven Heterojunction Photocatalyst Design with Continuously Adjustable Band Gap Materials. *The Journal of Physical Chemistry C*, 122(49)Pp., 28065–28074. <https://doi.org/10.1021/acs.jpcc.8b08060>
- Zwijenburg, M. A., 2022. The effect of particle size and composition on the optical and electronic properties of CdO and CdS rocksalt nanoparticles. *Physical Chemistry Chemical Physics*, 24(36)Pp., 21954–21965. <https://doi.org/10.1039/d2cp01342h>

